Molecular Crystals and Liquid Crystals
Publication details, including instructions for authors and subscription information:
http://www.tandfonline.com/loi/gmcl16

Dislocation Effects on the Viscoelastic Properties of a Smectic A Liquid Crystal

R. Bartolino [a b] & G. Durand [a]
[a] Laboratoire de Physique des Solides-Université de Paris-Sud, Bât. 510-91, 405, Orsay, France
[b] Universite di Roma, Istitudo di Fisica di Ingegneria, Roma, Italia
Version of record first published: 21 Mar 2007.

To cite this article: R. Bartolino & G. Durand (1977): Dislocation Effects on the Viscoelastic Properties of a Smectic A Liquid Crystal, Molecular Crystals and Liquid Crystals, 40:1, 117-132

To link to this article: http://dx.doi.org/10.1080/15421407708084475

Mol. Cryst. Liq. Cryst., 1977, Vol. 40, 117–132

Printed in Holland

Dislocation Effects on the Viscoelastic Properties of a Smectic A Liquid Crystal†

R. BARTOLINO‡ and G. DURAND

Laboratoire de Physique des Solides§—Université de Paris-Sud, Bât. 510-91 405 Orsay, France

(*Received November 12, 1976*)

We study the influence of defects on the viscoelastic properties of a smetic A liquid crystal (the octyloxycyanobiphenyl), by means of the undulation instability technique under a dilative stress. We introduce layers edge dislocations by using a wedge geometry. In this geometry, we predict the Burgers vector of the edge dislocation to increase with the wedge angle, so that the periodic pattern of the edge dislocations keeps a maximum wave number, of the order of the undulation instability wave number. We measure the undulation threshold and the short damping time τ of the elastic response to a step-like dilation, versus the wedge angle θ. The threshold is found to increase strongly with θ; for large θ this is well explained by a recent model from Pershan and Prost. At low θ our values tend toward the penetration length of de Gennes. The damping time shows at large θ a decrease $\tau \sim \theta^{-1}$, well described by a simple model. At small θ, we observe large oscillation of τ for periodic values of θ. This observation is explained by a geometrical coincidence of the wave length of the undulation instability and of the periodic pattern of edge dislocations in the wedge. These data are compatible with our model for the Burgers vector adjustment. Such a periodic pattern of low Burgers vector is the smectic analog of the Grandjean–Cano lines in cholesterics.

INTRODUCTION

Smectic liquid crystals have raised special interest because of their peculiar elastic properties. De Gennes has made predictions[1] on the anisotropy of elasticity in ideal smectics. Because these materials possess a regular layered

† Work supported by the French D.G.R.S.T. under contract N 650-892.
‡ On leave from Universita di Roma, Istituto di Fisica di Ingegneria, Roma, Italia.
§ Laboratoire associé au C.N.R.S.

texture, they should present a solid like elasticity for strains normal to the layers. As there is no ordering of molecules inside the layers (at least in the simplest A phase on which we restrict our interest here), strains inside the layers, giving rise to layer undulations, should be described by a curvature elasticity analogous to the one describing curvature distorsions in nematic liquid crystals. A natural length λ appears in the problem, which defines the scale over which a curvature strain stores as much energy as a compressional strain of equal amplitude; this penetration length λ introduced by De Gennes is of the order of a layer thickness. Experimental studies[2–5] have verified this symmetry related anisotropy of the elastic response of real smectic materials to small perturbations. However, an important result of these studies is the very short time during which one can observe an elastic response of a smectic liquid crystal to an applied strain normal to the layers. Usually a few tens of milliseconds after the application of the strain, the smectic material keeps a permanent plastic distortion, probably because of defect motion in the sample. Another unexpected result on smectic elasticity is the low experimental value of the critical exponent describing the temperature dependence of the penetration length close to a quasi second order smectic A $\rightarrow$ nematic phase transition. The discrepancy (0.16 compared to the predicted 0.33), confirmed by various experimental techniques in different groups,[5–7] is beyond experimental errors. These two open questions could be explained by the influence of defects in real smectics. They motivate further work on the interaction of texture defects on the elastic properties of smectic liquid crystals.

A theoretical approach of the role of defects on smectic elasticity has been made by Pershan[8] and Pershan and Prost[9] using an analog of the Peach–Koehler model for crystals. One of their predictions is a renormalization of the smectic elastic constant versus defect density which, coupled with defect mobility, appears as the important parameter of the problem. The purpose of the work presented in this paper is to measure elastic constant and elastic relaxation time versus defect density, in smectic materials. To start with, we need to prepare samples of known and variable defect concentration. Two methods could be used: first, to dissolve in the sample a controlled amount of impurities, the second to induce defects through the sample geometry, using a wedged cell for instance. In this work, we have chosen the second method. To measure the penetration length, we use the dilation instability technique described by Ribotta *et al.*[10,13] and Clark.[7] The principle of this experiment is recalled in part I where we also review what is known on the visco-elastic properties of smectic A and sketch a simple model to predict the Burgers vector of dislocations in a wedge. In part II we describe our experimental set up. Our experimental results are reported and discussed in part III.

I PRINCIPLE OF THE EXPERIMENT

a The buckling instability

Let us recall the buckling instability effect;[2,11,12] an homeotropic sample of smectic A is prepared in a glass cell of thickness d (Figure 1a). As explained in part II, we can increase d by a small quantity δ. This dilation δ results in a uniform strain δ/d measured along $0z$ normal to the layers, $0x$ being parallel to the layers. The dilation free energy density can be written as:

$$F = \frac{1}{2} B\left\{\left[\frac{\delta}{d} - \frac{1}{2}\theta^2\right]^2 + \lambda^2\left(\frac{\partial\theta}{\partial x}\right)^2\right\} \tag{I.1}$$

where B is the solid-like elastic constant and λ the penetration length; θ is an eventual tilt of the layers compared to $0x$. The θ^2 term expresses the fact that at constant layer number, a tilt results in a layer compression; the $\frac{1}{2}$ factor comes from a simple geometrical model of rigid rod molecules. Below a threshold dilation $\delta_{th} = 2\pi\lambda$, the system is expected to remain in a stressed homeotropic geometry. Above δ_{th}, the layers undulate to compensate by their tilt the applied stress. The undulation has a wave vector q_c defined by $q_c^2 \lambda d = \pi$. (Figure 1b).

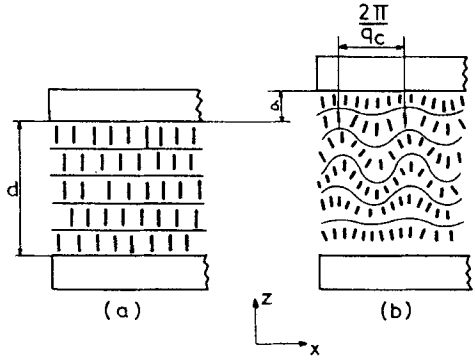

FIGURE 1 Schematic representation of the "buckling" instability. a) Undistrubed homeotropic smectic A sample of thickness d. b) The layers undulation appears after a dilation $\delta > \delta_{th}$.

The undulation instability can easily be observed through its light scattering properties. Illuminating the sample with a laser beam, the threshold of the undulation instability corresponds to a sharp increase of scattered light in a direction defined by the light momentum transfer equal to $\mathbf{q}_c$. The time evolution of the scattered intensity at constant applied strain above threshold gives informations on the undulation strain relaxation in the sample. Ribotta *et al.*[10,12,13] has observed that this relaxation happens in

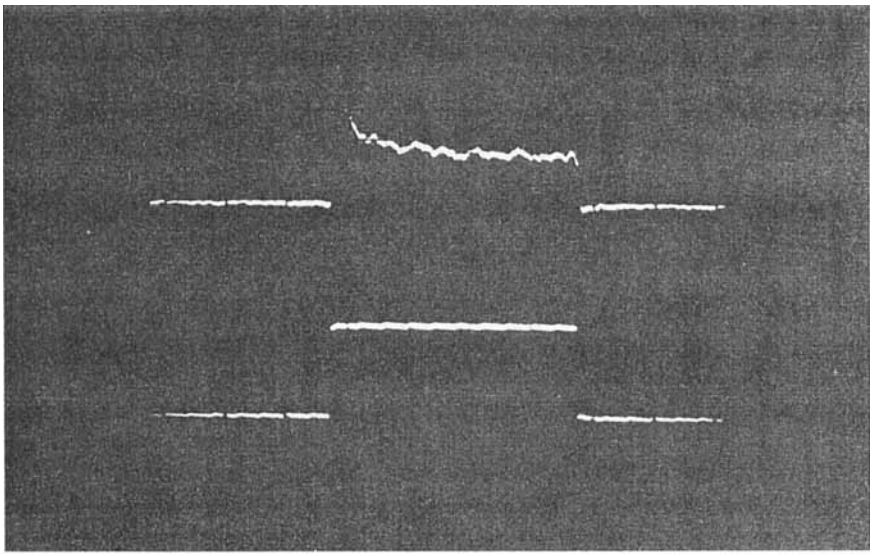

FIGURE 2 A typical optical signal undulation from the instability. A "peak" is visible, with decay time τ, a "plateau" follows. The lower signal is the applied voltage on the ceramics.

two steps: slightly above threshold, the optical signal (and then the molecular tilt) has the shape of a "peak". It relaxes down to zero with a short decay time τ_1 (a few tens of m sec). For higher dilations, the rapid relaxation is incomplete; the optical signal shows a "plateau" (see Figure 2) with a decay time τ_2 of the order of a few seconds. Microscope observations[10,12] have shown a correlated slow motion of dislocations emitted by the sample boundaries or gross bulk defects, which could explain the long time τ_2. It has been suggested[13] that the short relaxation process could be due to motion of dislocations already presented in the observed region of the sample. An unexplained result between the two relaxation regimes is the difference between the "peak" and the "plateau" threshold δ_1 and δ_2. Which one corresponds to $\delta_{th} = 2\pi\lambda$? Note that Clark[7] has not been able to observe the short relaxation process, since he applied to the smectic sample a too slowly varying dilation in the form of a linear ramp.

b Influence of defects

Assume a defect-free smectic sample between two parallel perfectly plane glass plates of layer thickness a. When tilting the plates to form a wedge of angle θ, one breaks the layers and creates an array of edge dislocations, of linear density $\Delta\rho_\theta$. Calling $\bar{l}$ the average horizontal ($0x$) distance between dislocations, the geometrical layer matching condition (Figure 3) gives

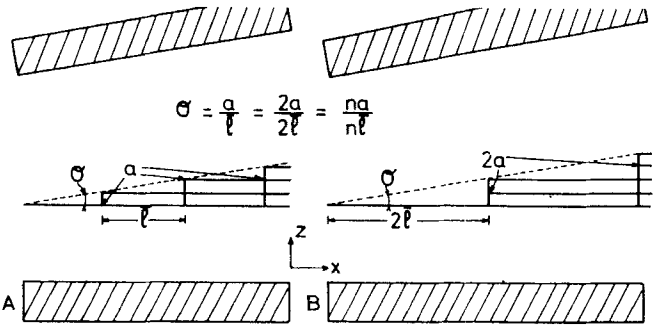

FIGURE 3 Schematic representation of two possible adjustments between the wave number q_θ and the Burgers vector $b = a$ or $b = 2a$ in the wedge geometry.

obviously $\Delta\rho_\theta = 1/\bar{l} = \theta/na$ for dislocations of Burgers vector length $b = na$ along $0z$. Layer dislocations are expected to be located close to the central region of the wedge, since they are strongly repulsed from their "mirror" image[8] beyond the plates. Dislocations should then make a more or less regular pattern of wave vector $q_\theta = 2\pi\Delta\rho_\theta = 2\pi\theta/na$ along the direction $0x$ of increasing thickness. This expected pattern should be the smectic analog of the Grandjean-Cano[19] lines observed in cholesterics.

Up to now, n is an unknown integer, presumably small for small θ. We can make a simple prediction on the dependence of the Burgers vector on the wedge angle θ. Let us assume that the core energy of a dislocation with $b = na$ is just the sum of the individual core energies of n simple dislocations with $b = a$; we could equally assume that these core energies are negligible compared to the free energy of the bulk distortion necessary to adjust the step-shaped dislocation to the plane boundaries of the wedge. Such an assumption is realistic.[14] For a given θ, we can choose all the possible $q_{\theta,n} = 2\pi\theta/na$ to match the wedge condition. Let us estimate the elastic free energy stored in the accompanying undulation distortion; the undulation amplitude is of the order of na. Distortion energy appears to be stored mainly in the mode of $q_z = \pi/d$, $q_x = q_{\theta,n}$. Its expression is given by the Fourier transform of Eq. (I.1):

$$\Delta F = \tfrac{1}{2}B[q_z^2(na)^2 + \lambda^2 q_{\theta,n}^4(na)^2]$$

$$= \tfrac{1}{2}B\left[\left(\frac{\pi}{d}\right)^2 a^2n^2 + \frac{\lambda^2(2\pi\theta)^4}{a^2n^2}\right] \tag{I.2}$$

For small dislocation density (more precisely for $q < q_c$), the splay nematic-like term is negligible compared to the layer compression term; F is minimum for the smallest possible n, i.e. $n = 1$. For larger angles, ΔF defined in formula

(I.2) is minimized when the two terms are equal. Writing $(\pi/d)^2 a^2 n^2 = \lambda^2(2\pi\theta)/a^2 n^2$ we find the condition:

$$q_{\theta,n} = q_c \tag{I.3}$$

Increasing θ from zero, this condition is fulfilled for:

$$\theta_{c,n} = n \cdot \frac{a}{2\pi}\left(\frac{\pi}{\lambda d}\right)^{1/2} = n\frac{a}{2\pi} q_c \tag{I.4}$$

with $n = 1, 2$ a.s.o. One expects to observe first a regular pattern of one layer dislocations for $0 < \theta < \theta_c = (a/2\pi)q_c$, then two layers dislocations appear more stable for $\theta_c < \theta < 2\theta_c$ and so on for n layers dislocations. For each wedge angle, there is an optimum Burgers vector such that the dislocation wave vector $q_{\theta,n}$ never exceeds q_c. Of course this model is oversimplified, by not taking into account the core structure of multilayer dislocation, nor the higher order elastic term in the highly distorted regions; its predictions should be at least qualitatively correct. Note that the grouping of dislocation with large Burgers vector has already been reported in an experiment of shear on smectic layers.[15,16]

In practice, a real smectic sample contains additional defects. For $\theta = 0$, we expect opposite sign layer dislocations to exist with unknown but equal densities $\rho^+ = \rho^- = \rho_0/2$. Some other defects are attached to the imperfection of the boundary glass plates. Increasing the wedge angle, the expected regular pattern of dislocation could be generated by an unbalanced density of bulk dislocations or by defects located on the boundaries. The periodic dislocation pattern predicted previously is probably only observable for low wedge angle. When θ is many times larger than θ_c, one expects the periodic pattern to blurr off. One enters the high defect density regime discussed by Pershan and Prost.[9] One of the predictions of their model is an elastic constant renormalization:

$$B = \frac{B_0}{1 + \alpha} \tag{I.5A}$$

B_0 is the defect free layer compression modulus. α is proportional to the defect density. This implies a λ renormalization in the shape:

$$\lambda = \lambda_0(1 + \alpha)^{1/2} \tag{I.5B}$$

In this large θ limit we can make also a prediction on the effect on the relaxation rate. We call the total density $\rho = \rho_0 + \Delta\rho_\theta$. In a simple picture, using the derivation from references 10 and 12 we can write

$$\tau_R \simeq \frac{\eta d}{Ba\rho\delta} = \frac{\eta d}{Ba\delta(\rho_0 + \Delta\rho_0)} \tag{I.6}$$

Where η is an effective viscosity. We shall try to fit our data on the two models, for large wedge angle.

c Relaxation mechanism

The undulation mode of smectics is overdamped. The observed peak in the undulation amplitude during the short time τ_1 after the application of a dilative step cannot be attributed to an inertial oscillatory effect. It has been attributed to a dissipative process involving plastic relaxation from defect motion. The observation of a relatively short time τ_1 indicates that this relaxation should involve local motion of initially existing defects (edge dislocations) which move over a mean distance $\bar{l} \sim 1/\Delta\rho$ comparable to, or smaller than the undulation wave, length $l_c = 2\pi/q_c$. These dislocations can overlap to give a uniform increase of layer number which compensates for the dilation. In absence of undulation, the dislocations move with the same velocity, whatever may be their orientation. In presence of undulation, the force acting on the dislocations should be locally modified by the periodic change in the stress from the undulation.

II THE EXPERIMENTAL SET-UP

The chemical compound we use is the octyloxycyanobiphenyl (BOON) which (X rays determined[1]) gives a layer thickness of $a = 30$ Å. Our measurements are made at the temperature of $T = 60°C$, well inside the smectic A phase (stable between 55°C and 67°C). The cell temperature is regulated by an electric oven, within 0.1°C. The cell is made of two glass plates optically polished at $\lambda/8$. Each plate is internally coated with a solution of polimerized silane,[18] to induce the homeotropic alignment. The cell thickness is typically $d = 175$ μm. This thickness defines a $\theta_c = 1.1\ 10^{-3}$ rad. The wedge angle can be adjusted by a system of screws represented on Figure 4. The angular range is limited by the elasticity of the holder from $-\theta_c$ to $+5\theta_c$. To measure

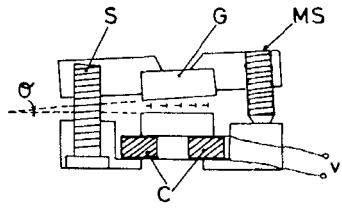

FIGURE 4 Tiltable wedge sample cell (C = ceramic ring, G = glass plates, S = steel screw, MS = micrometric screw, V = electric driving voltage).

the wedge angle, we illuminate the empty cell by a laser beam and measure the angle of the reflected beams. We identify the reflections from the inner faces of the plates by filling the cell with the liquid crystal and observing which reflected beams disappear because of index matching. Our accuracy of angle determination is estimated to be $\pm 10^{-4}$ rad. We can move one of the plates compared to the other with a ring-like piezoelectric ceramic (see Figure 4) on which an external voltage V is applied. The displacement δ is equal to 4.8 Å/volt, independent of the ceramic thickness. V is produced by a high voltage amplifier, following a low frequency (0.1 to 1 Hz) square wave generator. The rise time of the electric signal is less than 50 μsec. The range of applied voltage is typically 0–150 volt, giving a displacement range of 0–720 Å. The applied voltage has a constant polarity such that the displacement produced is always a dilation compared to the unperturbed state for zero applied voltage. To observe the undulation instability we use a light scattering set up previously described.[3] An extraordinary polarized 6328 Å laser beam enters the sample at an angle $\phi = 30°$ with the long axis of the molecules. The laser power is kept under 5 mW to prevent sample heating. The diffracted light by the layer undulation is ordinary polarized. This light should appear along a direction of space such that the momentum transfer wave vector is equal to q_c. There exist two directions of space which satisfy this relationship.[12] ϕ has just been chosen so that the two diffraction vectors $\mathbf{q}_c$ are orthogonals. By rotating the cell in the oven, we can adjust the wedge to align its axis along one of these diffraction vectors, then perpendicular to the other. The time varying intensity of the diffracted signal along each spot is detected by a phototransistor followed by a memory oscilloscope.

III EXPERIMENTAL RESULTS

As previously observed,[12] threshold determinations are a little ambiguous, when defects are present in the sample. This is obviously the case with our wedge sample. We fix to 0.1 Hz the frequency of the square wave voltage applied on the ceramics. With a large enough periodic dilation applied, we can visualize on a screen the two Bragg spots corresponding to the scattering by the undulation pattern.[2] These two spots are on the cone of allowed scattering for ordinary polarization. The measurement of the angular aperture of this cone, as explained in Ref. 3, gives us the value $n_e/n_0 = 1.10$ for the ratio of the extraordinary to ordinary indices for our compound at 60°C. From the Bragg spot position, we can deduce the wave vector $q_c = [2.7 \pm 0.2]10^4$ cm^{-1} using the methods explained in Ref. 12. From q_c we can deduce the value of λ, using the relationship $\lambda = \pi/q_c^2 d$. We have measured q_c and then λ for different wedge angles θ. q_c and λ seem to be

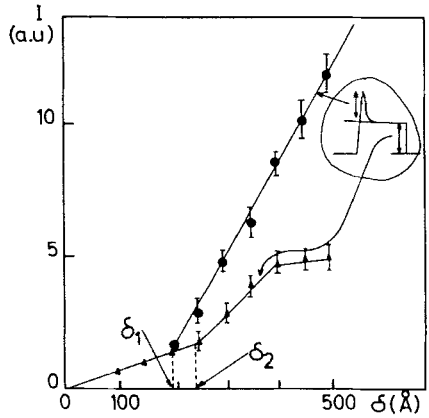

FIGURE 5 Typical scattered light intensity versus dilation. The full dots represent the peak intensity, the triangles the plateau intensity. The arrows indicate the two corresponding selected values for the threshold δ_1 and δ_2. The insert is a schematic representation of Figure 2.

almost independent of θ. The one noticeable point is a broadening of the spots which appear at large θ as portions of ellipses along the cone of allowed scattering. This broadening results in a larger error bar on the deducted values of λ. On Figure 6, one finds typically $\lambda = 21$ Å $\pm$ 3 Å for $\theta = 0$ and $\lambda = 24$ Å $\pm$ 6 Å for $\theta > 10^{-3}$ rad. We fix now our phototransistor on one (or the other) Bragg spot and record the time dependence of the observed Bragg scattered intensity. As the center of these spots do not change much when we vary θ, we have not to modify the position of the detector when adjusting the wedge angle. We define the "peak" and the "plateau" thresholds by the intersection of the initial undulation intensity (Figure 5) with the linear part of, respectively, the "peak" and of the "plateau" intensity curves. We do not extrapolate these lines down to the base line because we think that in the illuminated area, different regions contribute to the initial undulation signal, or to the instability signal.

a Threshold of the peak δ_1

We observe the light scattered by the undulation of wave vector $\mathbf{q}_c$ parallel to $\mathbf{q}_\theta$. For each angle θ of the wedge, we measure the dilation δ_1 corresponding to the appearance of the first peak of the optical signal. Our results are shown on Figure 6 (full dots). Going to negative and positive values of θ, we can observe that δ_1 is independent of the wedge angle close to $\theta = 0$. More generally δ_1 appears to be an even function of θ. Going to larger values of θ, we observe a spectacular increase of δ_1; this increase becomes significant for $\theta \sim 10^{-3}$ rad, i.e. for $\theta \sim \theta_c$. Within our experimental accuracy we

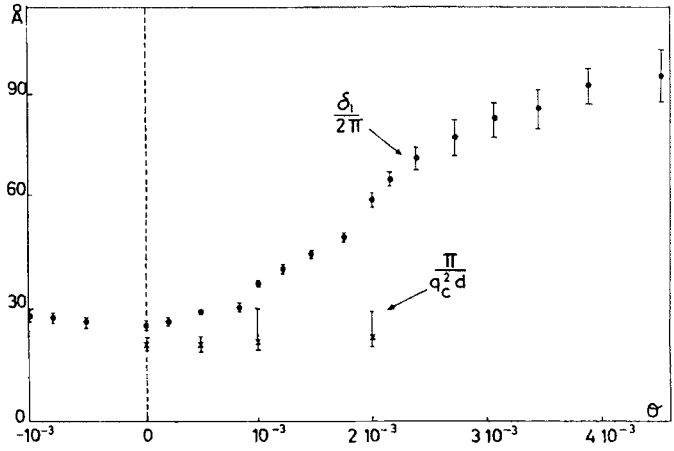

FIGURE 6 Comparison between the value of $\delta_1/2\pi$ and the value of $\pi/q_c^2 d$ versus θ. The de Gennes penetration length λ_0 corresponds probably to the lowest value at $\theta = 0$.

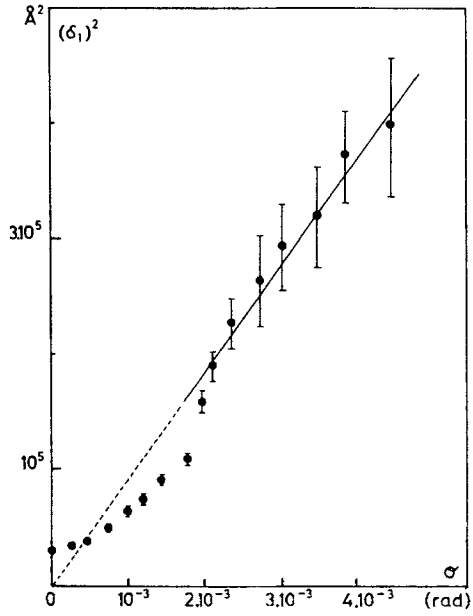

FIGURE 7 Square of the dilation threshold $(\delta_1)^2$ versus the tilt angle. The low angle values are not explained by the model of Ref. 9 (straight line).

cannot say if the small undulations of this curve, around the values $n\theta_c$ ($n = 1, 2, \ldots$) are significant. Defining always the penetration length in presence of defects by the expression: $\lambda = \delta_1/2\pi$, we conclude that the smectic texture becomes significantly softer for a defect linear density $\Delta\rho \sim q_c/2\pi = 4.310^3$ cm^{-1}. In the large angle limit we observe that δ_1 (and λ) shows a parabolic behavior versus θ. We have plotted on Figure 7 the square of δ_1 versus θ. For θ larger than about 2.10^{-3} rad, $(\delta_1)^2$ appears to be a linear function of the wedge angle, then of the dislocation density. This behavior is in agreement with formula (I.5B). At lower angles, our data do not follow the straight line which can simply be explained because Ref. 9 model is not valid for low defect density. We do not have yet any model to describe the observed increase of threshold in this low defect density regime. We should note however that the $\theta = 0$ value of $\delta_1/2\pi$ is equal to 24 Å $\pm$ 2 Å. This value is already a little larger than the 21 Å $\pm$ 3 Å deduced from the q_c observation. It is very likely that the defects present in the sample at $\theta = 0$ have already decreased the smectic elastic constant B, then have increased λ. For a reason we do not yet understand, the undulation threshold seems very sensitive to the defects density, although the optimum undulation wave vector is not. The best value of a defect independent λ_0 should be in that case the one deduced from the q_c observation $\lambda_0 = 21$ Å $\pm$ 3 Å. It would be interesting to look for the temperature dependence of λ_0 from the q_c observation, to see if the critical exponent found close a second order smectic A $\leftrightarrow$ nematic phase transition becomes closer to the predicted 0.33 value.

b Threshold of the plateau δ_2

We have just a few data on the plateau threshold δ_2. They are not reproducible as well as the δ_1 data. We observe that the plateau appears for a dilation systematically larger than the peak threshold. This systematic increase reinforces our belief that the peak threshold δ_1 is the correct one for the undulation instability. In Figure 8 we have plotted the difference of threshold $\delta_2 - \delta_1$ versus the wedge angle θ. This difference increases with θ but shows relative minima for $\theta = 0$, $\theta = \theta_c$, $\theta = 2\theta_c$. It seems experimentally that, when $q_\theta = q_c$, the wedge induced dislocations are less efficient to relax by their motion the dilative stress toward a state of zero undulation; we can imagine that because the wedge dislocations have the same period as the undulation, they are trapped, for large enough undulation amplitude, in the regions of largest local dilative stress. Depending if we have applied dilations larger than δ_2 or of values between δ_1 and δ_2, the plasticity associated to dislocation motion could imply a final state with large undulation amplitude in the first case of larger dilation, or a state without undulation in the second case at lower dilation.

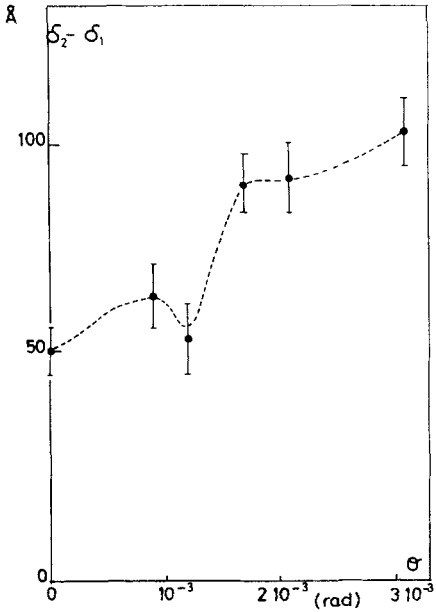

FIGURE 8 Difference between plateau and peak threshold ($\delta_2 - \delta_1$) versus θ.

c Decay time measurements

We analyse the decaying part of the peak as an exponential decay down to zero or down to the "plateau" amplitude, which appears time independent on Figure 4 because τ_2 is much larger than the sweeping time of the oscilloscope. The decay time of the peak τ_1 has been measured versus the wedge angle θ, for the diffracted beams corresponding to $\mathbf{q}_\theta \parallel \mathbf{q}_c$ and $\mathbf{q}_\theta \perp \mathbf{q}_c$.

1. $\mathbf{q}_\theta \perp \mathbf{q}_c$ Our result for τ_1 are plotted as open dots on Figure 9. Around $\theta \sim 0$, τ_1 appears to be constant, although for larger values of the wedge angle ($\theta > \theta_c$), we observe a regular $1/\theta$ like decrease of τ_1. This seems in qualitative agreement with the formula (I.6), but a numeric interpretation of the data is not easy. In this configuration the two patterns of distortion ($\mathbf{q}_c$) and of defects ($\mathbf{q}_\theta$) are orthogonals. That part of the forces on the wedge dislocations coming from the local undulation induces a non-uniform speed of propagation for different points of the same dislocation line. The situation is quite complicated. From the experimental data we can evaluate just an order of magnitude for the linear density of the initially present defects, of the order of $\rho_0 = 3.10^3$ cm^{-1} which is in agreement with independent qualitative estimations.[11]

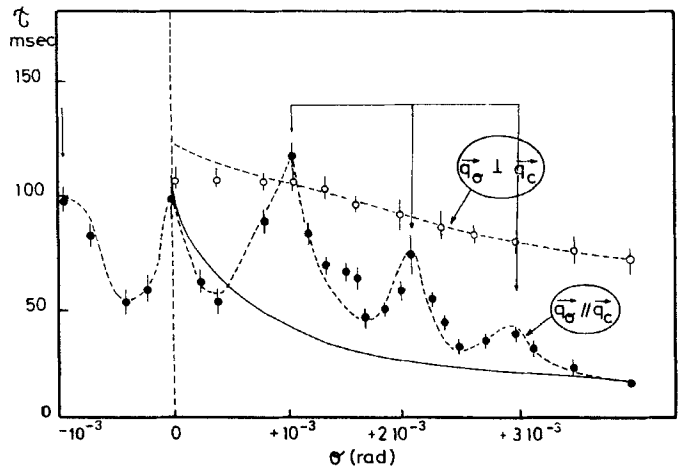

FIGURE 9 Decay time τ_1 versus θ in the two orientations of edge dislocation wave number $\mathbf{q}_\theta$ compared to the undulation wave number $\mathbf{q}_c$. The resonances for the integer multiples of $\theta_c = 1.1\ 10^{-3}$ rad. are typical of a geometrical coincidence between defect and undulation periodicity (see text).

2. $\mathbf{q}_\theta \perp \mathbf{q}_c$ The values of τ_1 corresponding to this configuration are indicated by full dots on Figure 7. One observes now quite a different behavior; also τ_1 decreases regularly when θ increases; in addition one observes large oscillations of τ_1 under the previously observed values. The oscillations are separated by four "resonances" of τ_1, for which the relaxation time seems to be quite the same as in the perpendicular configuration. The values of θ for these resonances are $\theta_0 = 0, \theta_1 = 1.1\ 10^{-3}$ rad, $\theta_2 = 2.1\ 10^{-3}$ rad, $\theta_3 = 3.2\ 10^{-3}$ rad. They appear to be the first integer multiples of $\theta_c \sim 1.1\ 10^{-3}$ rad. For these values of θ we have also observed a simultaneous increase of the static Rayleigh scattered signal in absence of applied dilation. The last observation indicates that for $\theta = n\theta_c\ (n = 1, 2, 3)$ the edge dislocations have a similar periodic pattern of wave vector q_c. This result is in agreement with our prediction of part I that the Burgers vector should vary with θ to force q_θ to remain at values around q_c at large θ. To ascertain the point, we should make a systematic angular analysis of the scattered light by the static undulation for values of θ different from θ_c We shall make such an analysis in the future. For this configuration, despite the presence of local variations of the force acting on edge dislocation, each defect moves with a uniform velocity. In the large θ limit, we can try to fit our data with the formula (I.6). The fitted curve is shown in Figure 9. This fit gives an estimate of the ratio $\rho_0/(\rho_0 + \Delta\rho_0)$. This gives an independent value of $\rho_0 \simeq 4.10^{-3}$ cm^{-1} in agreement with the previous one found. We can also simply explain why in the two configurations ($\mathbf{q}_\theta \| \mathbf{q}_c$, $\mathbf{q}_\theta \perp \mathbf{q}_c$) the relaxation times are equal for

$\theta = -n\theta_c$. Our observations suggest that, for these "resonances", the periodic pattern of wave vector $q_\theta = q_c$ is less sensitive to the uniform part of the forces induced by the dilation, because of some compensation from the local stresses coming from the undulation deformation. Figure 10 shows a

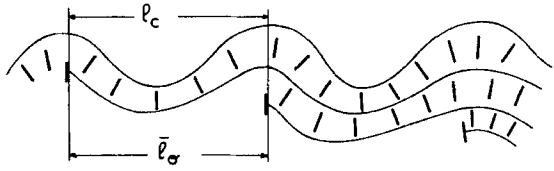

FIGURE 10 Schematic description of the "trapping" between the dislocation pattern and the undualtion when $q_\theta = q_c$.

possible configuration of dislocation which is placed compared to the undulation in such a position. For all other wedge angle, $|q_c|$ and $|q_\theta|$ are different, there cannot be such a spatial concordance; the dislocation pattern feels at random the additional stresses from the layer undulation. Individual dislocations move faster and the relaxation time τ_1 decreases. This explains the periodic observed lobes in the $\tau_1(\theta)$ experimental curve of Figure 9.

d Threshold difference ($\delta_2 - \delta_1$) versus decay time

As explained previously the difference between the two thresholds δ_1 and δ_2 shows some dispersion. A question of interest is to see if there is any correlation between this difference and the relaxation time τ_1. A simple model would predict that the number of additional layers which can be relaxed is proportional to the number of available dislocations. In consequence τ_1 should be inversely proportional to $[\delta_2 - \delta_1]$. We have plotted on Figure 11 our data for the threshold difference $(\delta_2 - \delta_1)$ versus τ_1. We first notice that the $\delta_2 - \delta_1$ values seem to group around values like 50 Å, 80 Å, 120 Å, 170 Å. These values are almost equally spaced by a quantity of about 40 Å, of the order of the typical X-ray determined layer thickness $a = 30$ Å. The other point is that no reproducible data exist which give a value of $(\delta_2 - \delta_1)$ smaller than one layer thickness a, which is obviously the minimum amount of dilation that can be relaxed by a dislocation of Burgers vector of one layer; τ_1 appears inversely proportional to $(\delta_2 - \delta_1 - a)$. This observation is a proof of the existence of one layer dislocation in our wedge sample; we do not know, however, if these dislocations are induced by the wedge or are already present at $\theta = 0$.

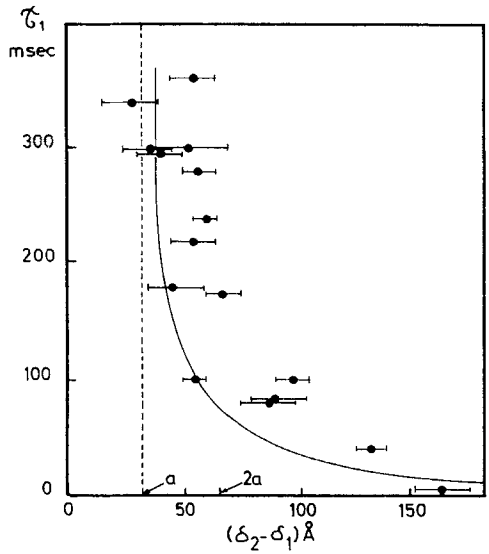

FIGURE 11 Threshold difference $\delta_2 - \delta_1$ versus the decay time τ_1. Note that this difference is larger than 30 Å, the physical thickness of one layer.

CONCLUSIONS

We have measured the undulation instability threshold of a smectic A liquid crystal placed in a wedge of variable angle. We have first observed a large increase of the apparent penetration length λ versus the wedge angle, i.e. the edge dislocation density. At large density, λ follows the prediction of a model from Pershan and Prost. Surprisingly, the undulation wave vector seems not to depend on defect density and give a better determination of λ. We believe that systematic measurements of λ versus temperature and defect density should give the "real" value of the penetration length, which should follow the predicted critical exponent close to a smectic A to nematic second order phase transition. The decay time measurements show very large oscillations versus the wedge angle. These oscillations appears for periodic values of θ. We have attributed these oscillations to spatial resonances between the wedge induced pattern of edge dislocations and the undulation mode. This is the first observation of the smectic analog of the Grandjean–Cano edge dislocations in cholesterics. This smectic periodic dislocations seem to adjust their Burgers vector so that their wave number remains around the value q_c of the natural undulation wave number in the sample. This is in agreement with our prediction which explains this optimum value of Burgers

vector by the repulsion of dislocation, in term of stored elastic energy in the bulk. We have also proved the existence of "one-layer" dislocations in the wedge. Most of the work remains to be done to explain the details of the motion of a single dislocation in presence of an undulation instability. However the analysis of the local stresses is possible. Coupled stress-strain measurements should be done in the future. These measurements are very simplified by the short time scale of duration of the elastic response in these soft materials. We believe that smectic liquid crystals can be interesting models to study the relationship between the microscopic properties of lamellar materials and their plastic behavior.

References

1. P. G. de Gennes, *J. de Phys.*, **30 C-4**, 65 (1969).
2. M. Delaye, R. Ribotta, and G. Durand, *Phys. Lett.*, **44A**, 139 (1973).
3. R. Ribotta, G. Durand, and D. Litster, *Solid State Comm.*, **12**, 27 (1973).
4. R. Ribotta, D. Salin, and G. Durand, *Phys. Rev. Lett.*, **32**, 6 (1974).
5. H. Birecki, R. Shaetzing, F. Rondelez, and D. Lister, *Phys. Rev. Lett.*, **36**, 1376 (1976).
6. R. Ribotta, *C. R. Acad. Sci.*, **279B**, 295 (1974).
7. N. A. Clark, *Phys. Rev.*, **A14**, 1551 (1976).
8. P. S. Pershan, *J. Appl. Phys.*, **45**, 1590 (1974).
9. P. S. Pershan and J. Prost, *J. Appl. Phys.*, **46**, 2343 (1975).
10. R. Ribotta and G. Durand, to be published in *J. de Physique* (Feb. 1977).
11. N. A. Clark and R. B. Meyer, *Appl. Phys. Lett.*, **22**, 10 (1973).
12. R. Ribotta, Thesis, Orsay (CNRS A 1450) 1975.
13. R. Ribotta, Les Houches lecture note (1973), Ed. R. Balian, Gordon & Breach.
14. C. Williams, Private communication.
15. C. Williams and M. Kleman, *J. de Physique*, **36 C-1**, 315 (1975).
16. C. Williams, Thesis, Orsay (CNRS A 01 2720) (1976).
17. J. E. Lydon and C. J. Coakley, *J. de Physique*, **36 C-1**, 45 (1975).
18. F. J. Kahn, *Appl. Phys. Lett.*, **22**, 386 (1973).
19. R. Cano, *Bull. Soc. Franc. Mineral.*, **91**, 20 (1968).